Taylor & Francis
Taylor & Francis Group

ORIGINAL ARTICLE

Check for updates

Effect of spatial distribution of boron and oxygen concentration on DNA damage induced from boron neutron capture therapy using Monte Carlo simulations

Jie Qi[a], Changran Geng[a,b,c], Xiaobin Tang[a,b,c], Feng Tian[a], Yang Han[a,d], Huan Liu[a], Yuanhao Liu[a], Silva Bortolussi[d], and Fada Guan[e]

[a]Department of Nuclear Science and Technology, Nanjing University of Aeronautics and Astronautics, Nanjing, China; [b]Key Laboratory of Nuclear Technology Application and Radiation Protection in Astronautics, Ministry of Industry and Information Technology, Nanjing, China; [c]Joint International Research Laboratory on Advanced Particle Therapy, Nanjing University of Aeronautics and Astronautics, Nanjing, China; [d]Department of Physics, University of Pavia, Pavia, Italy; [e]Department of Radiation Physics, Division of Radiation Oncology, The University of Texas MD Anderson Cancer Center, Houston, TX, USA

ABSTRACT

Purpose: This paper aims to investigate how the spatial distribution of boron in cells and oxygen concentration affect the DNA damage induced by charged particles in boron neutron capture therapy (BNCT) by Monte Carlo simulations, and further to evaluate the relative biological effectiveness (RBE) of DNA double-strand breaks (DSBs) induction.

Materials and methods: The kinetic energy spectra of α, ^{7}Li particles in BNCT arriving at the nucleus surface were obtained from GEANT4 (Geant4 10.05.p01). The DNA damage caused by BNCT was then evaluated using MCDS (MCDS 3.10A).

Results: When α or ^{7}Li particles were distributed in the cytomembrane or cytoplasm, the difference in DNA damage of the same types was less than 0.5%. Taking the 137Cs photons as the reference radiation, when the oxygen concentration varied from 0% to 50%, the RBE of 0.54MeV protons and recoil protons varied from 5 to 2, whereas it decreased from 10 to 3 for α or ^{7}Li particles.

Conclusion: The RBE of DSB induction all charged particles in BNCT decreased with the increase of oxygen concentration. This work indicated that the RBE of different radiation particles of BNCT might be affected by many factors, which should be paid attention to in theoretical research or clinical application.

Introduction

As an advanced binary targeted therapy technology, boron neutron capture therapy (BNCT) has its unique physical and radiobiological advantage. The physical principle of BNCT is based on the production of low-energy and short-range α and ^{7}Li particles through the ^{10}B (n,α) ^{7}Li reaction which can deposit dose locally in the tumors. Compared with conventional photon-based radiotherapy, the high linear energy transfer (LET) characteristics of the charged particles generated in BNCT result in high relative biological effectiveness (RBE) in tumors (Barth et al. 2005; Moss 2014). The determination of biological dose distribution in patients is critical for practitioners to evaluate the therapeutic effects of BNCT. The biological dose calculation of BNCT is more complicated (Lin et al. 2011), because it includes multiple types of particles such as photons, protons, α and ^{7}Li particles, each of which has different RBE values. Therefore, the biological effects of all of the different radiation types in BNCT must

be considered to obtain the overall biological dose (Hiratsuka et al. 1991).

The biological effects of BNCT could be determined from biological experiments and mathematical modeling. Many previous studies have used the biological effectiveness values of different types of boron compounds estimated through animal experiments to calculate the BNCT biological dose. One study by Farías et al. has shown that the compound biological effectiveness (CBE) of boronophenylalanine (BPA) and sodium borocaptate (BSH) in tumors was 3.8 and 2.3, respectively (Morris et al. 1994; Farías et al. 2014). Meanwhile, many biological models have been developed including mechanistic and phenomenological models to calculate the biological effectiveness of charged particles. For example, Horiguchi et al. have applied the microdosimetric kinetic model (MKM) to estimate the alpha in the linear-quadratic model of cell survival curve (Hawkins 1998; Horiguchi et al. 2015). Sato et al. used the MKM model to investigate the relationship between the boron concentration and biological effects (Sato et al. 2018). Hu et al.

demonstrated that PHITS could be used in microdosimetry studies, as well as in assessing absorbed dose and biological effects in BNCT (Hu, Tanaka, Takata, Endo, et al. 2020). In addition, the underlying mechanism in biological systems has been investigated, such as ionizing radiation-induced base damage (BD), DNA single-strand breaks (SSBs) and double-strand breaks (DSBs) as well as the DNA damage repair pathways. For example, Nikjoo et al. reviewed how to link microdosimetric parameters to cell death and DNA damage (Nikjoo et al. 1991). Zhu et al. used the Monte Carlo application of TOPAS-nBio to analyze the effects of different physical and chemical processes or energy thresholds on DNA damage under proton irradiation (McNamara et al. 2017; Zhu, McNamara, McMahon, et al. 2020). Based on this study, they further used the MEDRAS repair model to analyze chromosomal aberrations (Zhu, Mcnamara, Ramos-Mendez, et al. 2020). Luo et al. used the Monte Carlo Damage Simulation software (MCDS 3.10 A) to calculate the yield of DNA damage induced by therapeutic protons (Luo et al. 2020).

However, the mechanism of radiation damage caused by BNCT has seldom been thoroughly studied for either normal or tumor cells. For the sake of simplification, many previous studies did not fully consider the radiosensitivity of cells and enrichment of boron compounds in determining the BNCT biological effects. In the present study, we aim to evaluate the biological effects of BNCT by taking into consideration of both physical interactions and radiobiological characteristics of BNCT. The method of combining GEANT4 and MCDS simulation to analyze radiation damage caused by charged particles in BNCT is proposed for the first time. The effects of the spatial distribution of boron in cells and oxygen concentration on the radiation-induced DNA damage and the RBE of DSB have been investigated.

Materials and methods

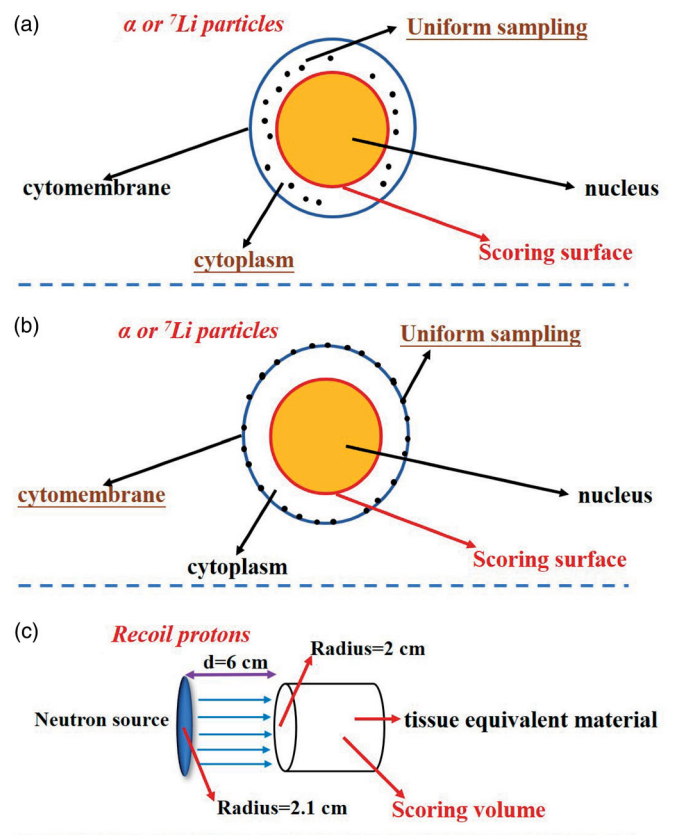### Particle source configuration in Geant4 Monte Carlo simulation

In BNCT, the types of charged particles mainly include α and ^7Li particles produced by the $^{10}B(n,\alpha)^7Li$ reaction, recoil protons produced by the capture of fast neutrons by hydrogen atoms, and 0.54 MeV monoenergetic protons generated from the capture of thermal neutrons by nitrogen atoms (Horiguchi et al. 2015).

In the current simulation process, based on the $^{10}B(n,\alpha)^7Li$ reaction, the radiation source corresponding to the boron dose was composed of two branches: (1) 1.47 MeV α particles and 0.84 MeV ^7Li particles with a branching ratio of 93.7%, and (2) 1.78 MeV α particles and 1.01 MeV ^7Li particles with a branching ratio of 6.3% (Karaoglu et al. 2018). Considering the spatial distribution of boron compounds in the cell, the initial emission positions of α and ^7Li particles were sampled according to the spatial distribution of boron compounds. At the same time, α and ^7Li particles were evenly distributed and emitted particles isotropically. The specific model configurations are shown in Figure 1(a,b). As shown in Figure 2, the radiation

source, recoil protons, is defined by an energy spectrum, which is calculated by irradiating the cylindrical tissue-equivalent material with a neutron source in Geant4 Monte Carlo Simulations (Geant4 10.05.p01) (Allison et al. 2016; Incerti et al. 2018). In our study, the neutron beam is based on the published energy spectrum of the Massachusetts Institute of Technology (MIT) epithermal reactor beam developed for BNCT (Kiger et al. 1999). Here, the components of tissue-equivalent material include H (10.1%), C (11.1%), N (2.6%), and O (76.2%) (Horiguchi et al. 2015). The radius of equivalent tissue material is set as 2 cm, the radius of neutron beam is set as 2.1 cm, the distance between neutron source and the surface of equivalent tissue material is 6 cm. The geometry of the simulation is shown in Figure 1(c). The G4EmStrandPhysics_option4, G4HadronElasticPhysicsHP, G4Decay, G4IonBinary CascadePhysics, G4StoppingPhysics, Geant4_HP_thermal and G4EmExtraPhysics are adopted in this study as described in previous studies (Geng et al. 2016), the detailed hadronic interaction category and physics models are listed in Table 1.

MCDS

At present, several studies have analyzed DNA damage through track structure simulations (Sakata et al. 2019; Tang et al. 2019; Sakata et al. 2020). However, the MCDS software

Figure 1. Models configuration in Geant4 Monte Carlo simulations. Process of recording the energy spectrum distribution of α or ^7Li particles arriving at the surface of nucleus when they were evenly distributed in the cytoplasm (a) or cytomembrane (b); process of recording energy of recoil protons in equivalent tissue material when it was irradiated by Massachusetts Institute of Technology (MIT) neutron source (c).
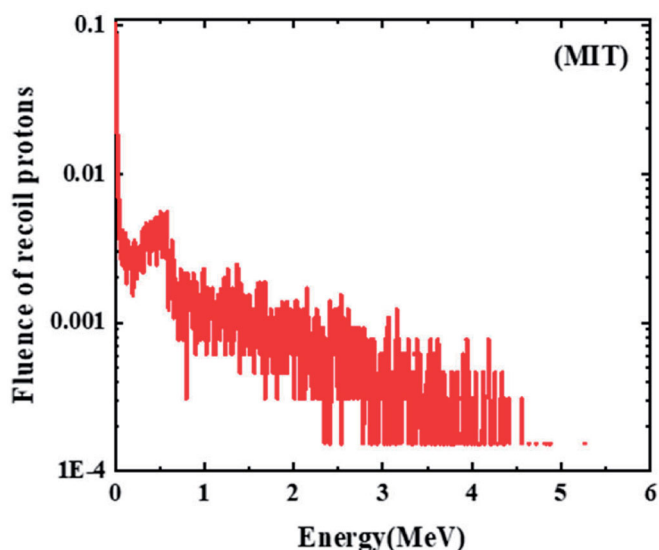
Figure 2. Energy spectrum of recoil protons in equivalent tissue material when it was irradiated by MIT neutron source using Geant4 simulations.

Table 1. The hadronic interaction category and physics models for neutrons, protons and alpha particles.

Particle types	Interaction category	Physics model
Neutron	neutronInelastic	NeutronHPInelastic
(<20 MeV)	nCapture	NeutronHPCapture
	nFission	NeutronHPFission
	hadElastic	NeutronHPElastic
Alpha	alphaInelastic	Binary Light Ion Cascade
(<4 GeV/n)	hadElastic	hElasticLHEP
Proton	protonInelastic	ParticleHPInelastic
(<200 MeV)	hadElastic	hElasticCHIPS

adopts a quasi-phenomenological model to compute particle- and energy-dependent DNA damage yields, the computation of which is much faster than some common particle track-structure simulations (Semenenko and Stewart 2004; Semenenko 2006; Chatzipapas et al. 2020). It should be noted that the MCDS only calculates the induced DNA damage without considering the DNA damage repair kinetics. The DNA damage induction dataset can be used as the input for other mechanistic biophysical models to calculate the biological effects. For example, the combined use of MCDS and the repair-misrepair-fixation (RMF) model have been applied in calculating the RBE of different ions (Frese et al. 2012; Kamp et al. 2017; Guan et al. 2018). Furthermore, the radiation damage induced by indirect ionizing radiation, such as photons and neutrons, is essentially caused by their secondary particles. Therefore, in MCDS, the calculation of DNA damage caused by incident photons or neutrons requires the kinetic energy spectra of secondary electrons or recoil protons as the input parameters (Semenenko and Stewart 2004; Semenenko 2006). In addition, MCDS can take into consideration the effect of oxygen concentration or the concentration of the free radical scavenger on the DNA damage from ionizing radiation (deLara et al. 1995). The DNA damage types and assessment methods used in the present work are shown in Table 2. Four adjustable parameters (i.e. segment length [n_{seg}], number of strand breaks [σ_{Sb}], BD to SB ratio [f], and minimum distance between clusters [N_{min}]) must be determined in

Table 2. Evaluation methods of the types of DNA damage in MCDS algorithm.

Cluster type	Assessment method
BD	One or more BD (no strand break)
SSB	Strand break (no auxiliary damage)
SSB+	Two strand breaks on the same strand
2SSB	Two or more strand breaks on opposite strands separated by at least 10 base pairs (bp)
DSB	Two strand breaks on opposite strands with a separation ≤10 bp
DSB+	Double-strand breaks accompanied by one (or more) additional strand breaks within 10 base pairs separation
DSB++	More than one double-strand break whether within the 10 base pairs separation or further apart

BD: base damage; SSB: single-strand break; DSB: double-strand break.

MCDS, which are determined by track-structure simulation (Semenenko and Stewart 2004; Semenenko 2006; de la Fuente Rosales et al. 2018), and primarily related to the particle type and kinetic energy. In the MCDS simulation, the radiation parameters (particle types, energies, radiation dose) were set according to the energy distributions obtained by Geant4 simulations. Oxygen concentrations 0%, 0.01%, 0.1%, 1%, 5%, 10%, 21%, and 50%, respectively, were set in the oxygen effect parameters. Normal O_2 concentration is above 21% in well oxygenated cells, and 50% O_2 concentration corresponds to 380 mmHg. In previous study, Luo et al. have analyzed the effect of 0.001–100% oxygen concentration on DNA damage in proton therapy (Luo et al. 2020).

Geometry configuration in Geant4 and MCDS simulations

In the current simulation work, considering the boron compounds enrichment difference in cells, the squamous tongue cancer cell is considered as a current research object, whose nucleus radius and cell radii are 3 μm and 5 μm, respectively. In Geant4 simulations, the material of cells is set as water for simplicity. In MCDS, the nuclear radius is also 3 μm.

RBE calculation

The RBE could be affected by many factors, such as radiation dose, dose rate, cell or tissue type, cell cycle, and biological endpoint (Okumura et al. 2013; Howard et al. 2017). In general, RBE is defined as the dose ratio of the reference radiation to the test radiation resulting in the identical radiation effect, that is, the same cell surviving fraction. In addition, the RBE can also be calculated for each type of DNA damage considered, among them, DSB is the most critical DNA damage related to reproductive cell death. The RBE for DSB induction can be defined as the dose ratio of the reference radiation to the test radiation with the same yield of DSB induction (Rothkamm and Löbrich 2003).

$$RBE_{DSB} = \frac{D_\gamma}{D_P} \qquad (1)$$

Here, P represents the type of test radiation to be studied, and γ is the reference radiation, usually photons. In this report, unless specifically pointed out, RBE from MCDS calculations refers to the RBE of DSB induction. Specifically, the distribution of DNA damage was simulated at the condition of different radiation doses. On this basis, by selecting the same number of DSBs, the ratio of the corresponding reference radiation dose to the required dose of the ion to be measured is the RBE_{DSB}.

In the cytoplasm, because of its thickness, when the particles are transported to the nucleus, a flat area is more likely to appear in the energy distribution, while the particles are emitted on the cytomembrane, because its geometry is only a thin surface, the peak shape is more likely to appear in the energy distribution of α and ^7Li particles. Considering that 0.54 MeV protons and recoil protons are already located in the nucleus, the original energy (refer to Figure 2 for the energy spectrum of recoil protons) has been used in the MCDS computations.

Results

### Effects of the boron enrichment difference on the yield of DNA damage

Energy spectrum of α and ^7Li particles entering the cell nucleus in Geant4 simulations

In Geant4 simulations, the initial emission positions of α and ^7Li particles are set as the cytoplasm or cytomembrane. The corresponding energy spectral distribution of α and ^7Li particles are scored on the surface of the nucleus (Figure 3).

Effects of the boron compounds enrichment difference on DNA damage for α and ^7Li particles in normoxic conditions in MCDS

The obtained energy spectra in Figure 3 were used as the input particle source parameter of MCDS simulations. In the environment of normal oxygen concentration (i.e. 21%), the number of clustered damage and yield of DNA damage with different complexities induced by α and ^7Li particles are shown in Figure 4.
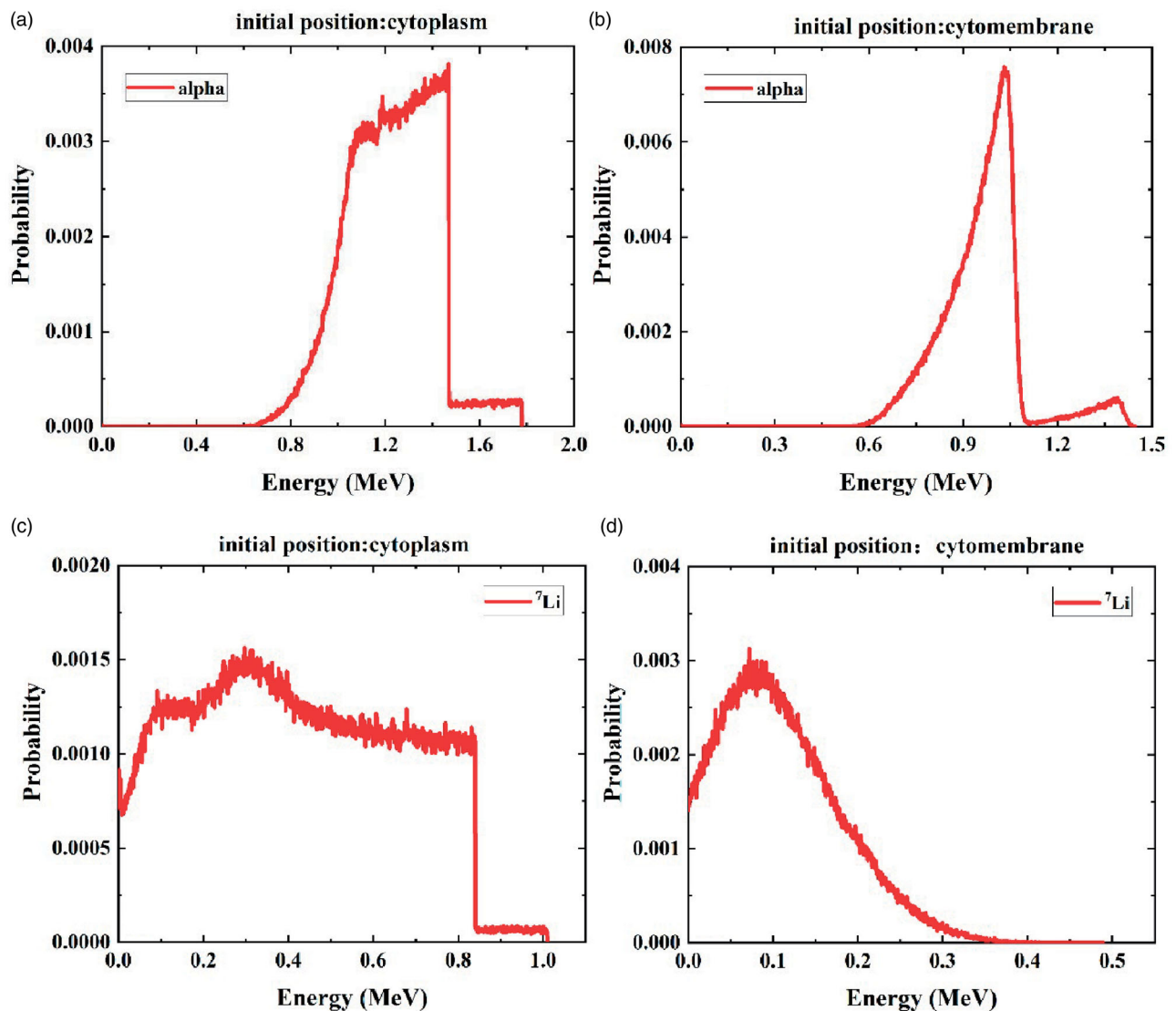
Figure 3. Energy spectra of α particles scored on the surface of the nucleus originating from the cytoplasm (a) or cytomembrane (b); the energy spectra of ^7Li particles scored on the surface of the nucleus originating from the cytoplasm (c) or cytomembrane (d).
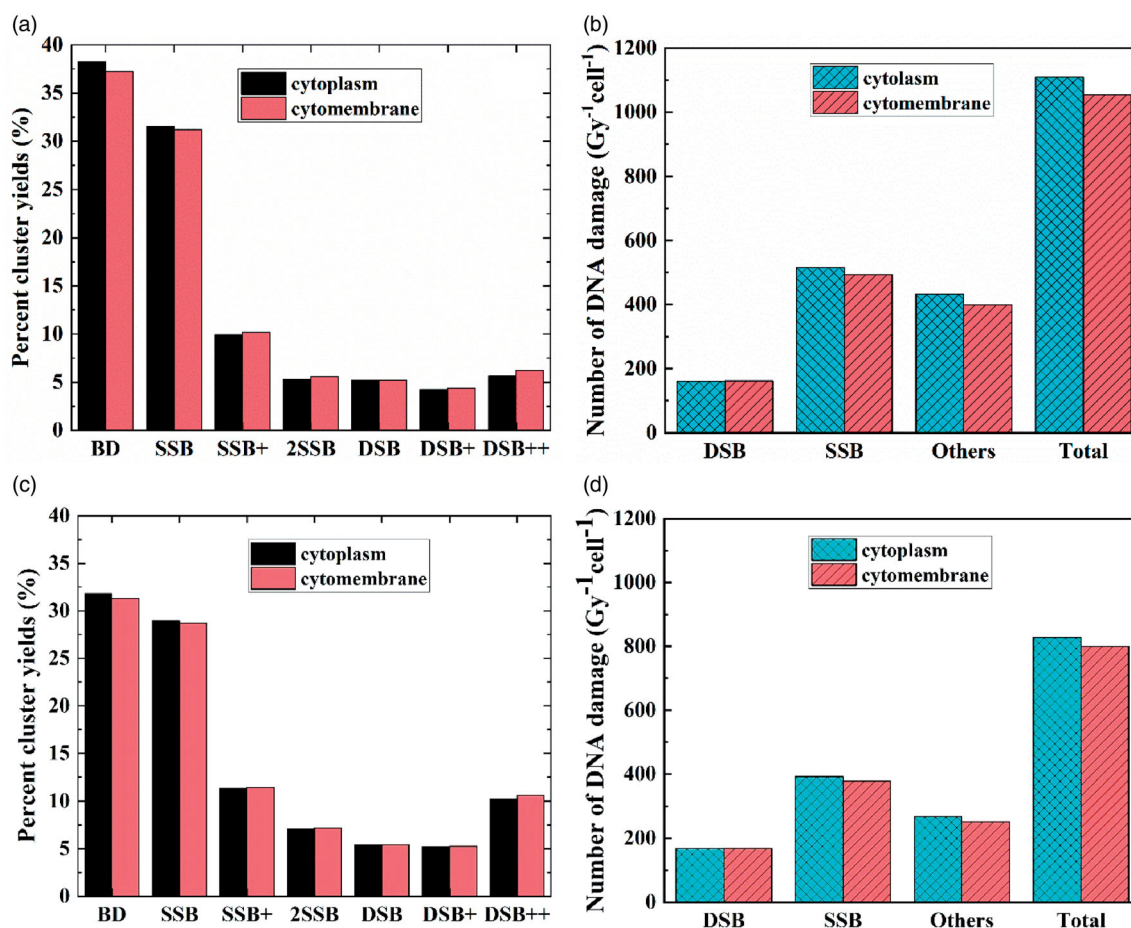
Figure 4. Percentage of DNA damage with different complexities and the number of clustered damage under normoxic conditions in MCDS algorithm. Panel (a) and (b) are the results from α particles. Panel (c) and (d) are from ^{7}Li particles.

Table 3. RBE of α and ^{7}Li based on two kinds of distribution of boron compounds in normoxic conditions.

	Location	RBE$_{DSB}$		Location	RBE$_{DSB}$
Alpha	Cytoplasm	3.27	^{7}Li	Cytoplasm	3.44
	Cytomembrane	3.31		Cytomembrane	3.45

When α or ^{7}Li particles are distributed in the cytomembrane or cytoplasm, the difference in the percentage of different types of DNA damage is not obvious, but simple damages (BD and SSB) and other more complex damages (including SSB+, 2SSB, DSB, DSB+, and DSB++) has opposite trends in these two distributions (Figure 4(a,c)). As shown in Figure 4(b,d), the number of DSB induced in the nucleus for the cytomembrane as the initial position is slightly higher than that for the cytoplasm as the initial position by 0.3%, but the number of SSB, other damages, and total damages emitting from the cytomembrane is slightly lower than that from the cytoplasm by 3.4%, 5.6%, 3.3%, respectively.

Effects of the boron compounds enrichment difference on RBE for α and ^{7}Li particles in normoxic conditions

Table 3 shows the RBE of α and ^{7}Li particles based on two kinds of distribution of boron compounds, that is, only in the cytoplasm or the cytomembrane, in normoxic conditions. The RBE of α and ^{7}Li particles for the cytomembrane

as the initial position is slightly higher than that for the cytoplasm as the initial position.

Effects of oxygen concentration on DNA damage and RBE for all charged particles of BNCT in MCDS

Effects of oxygen concentration on DNA damage for all charged particles of BNCT

Based on the energy spectra of α and ^{7}Li particles corresponding to Figure 2(a,c), in order to reduce the influence of other variables, the nucleus radius is still set to 3 μm. The numbers of DNA damage induced by all charged particles in BNCT under different oxygen concentrations are shown in Figure 5.

As shown in Figure 5(a,b), the number of SSB at the same oxygen concentration under the irradiation of α and ^{7}Li particles is higher than other damages. As the oxygen concentration of tumor cells increased, the number of damages induced by α and ^{7}Li particles remain basically unchanged. For the same initial distribution, the number of SSB, other damages, and total damages caused by α particles is higher than that of ^{7}Li particles.

For monoenergetic protons, when the oxygen concentration increases from 0.01% to 50%, the numbers of DSB, SSB and total clusters increase gradually, whereas the number of other damage clusters decreases slightly (Figure 5(c)). For
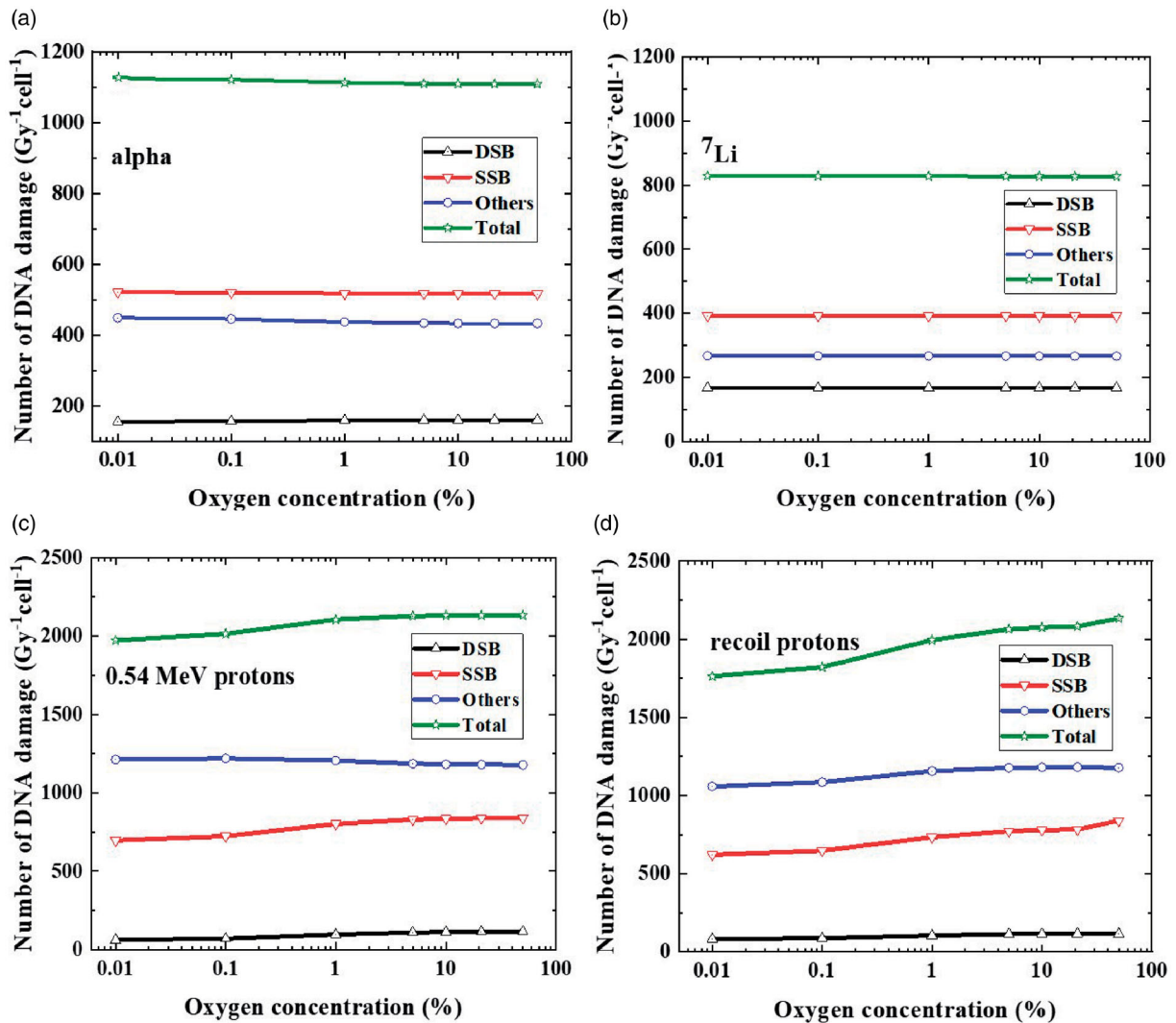
Figure 5. Number of DNA clustered damage under different oxygen concentrations caused by the radiation of α particles (a), ^{7}Li particles (b), 0.54 MeV protons (c), and recoil protons (d) calculated by MCDS.

recoil protons, the numbers of SSB and total DNA damages increase with the increase of oxygen concentration. However, when the oxygen concentration is 50%, the numbers of DSB and other damages decrease by 1.47% and 0.26%, respectively, compared with the results of oxygen concentration of 21% (Figure 5(d)).

DNA damage induced by reference radiation (i.e. ^{137}Cs) under different oxygen concentrations

In the MCDS algorithm, for neutral particles such as photons or neutrons, their secondary electrons or recoil protons should be set as the source term for DNA damage calculation. In the current study, ^{137}Cs photons are used as the reference radiation, whose secondary electrons energy spectrum is shown in Figure 6(a) (Hsiao and Stewart 2008). For ^{137}Cs photons, the number of DNA clustered damage

increases significantly with the increase of oxygen concentration (Figure 6(b)).

Effects of oxygen concentration on the RBE of all charged particles of BNCT

The RBE is calculated by taking α and ^{7}Li particles emitted from the cytoplasm with the cell nucleus radius of 3 μm set in MCDS. As shown in Figure 7, when the oxygen concentration is lower than 1%, the RBE of α and ^{7}Li particles decrease sharply with the increase of oxygen concentration. When the oxygen concentration is higher than 10%, the RBE is basically unchanged. The RBE of α and ^{7}Li particles is in the range of 3–10. For 0.54 MeV protons and recoil protons, the RBE remains basically unchanged when the oxygen concentration is higher than 5%. It is concluded that the biological effectiveness of BNCT on tumor cells exists a
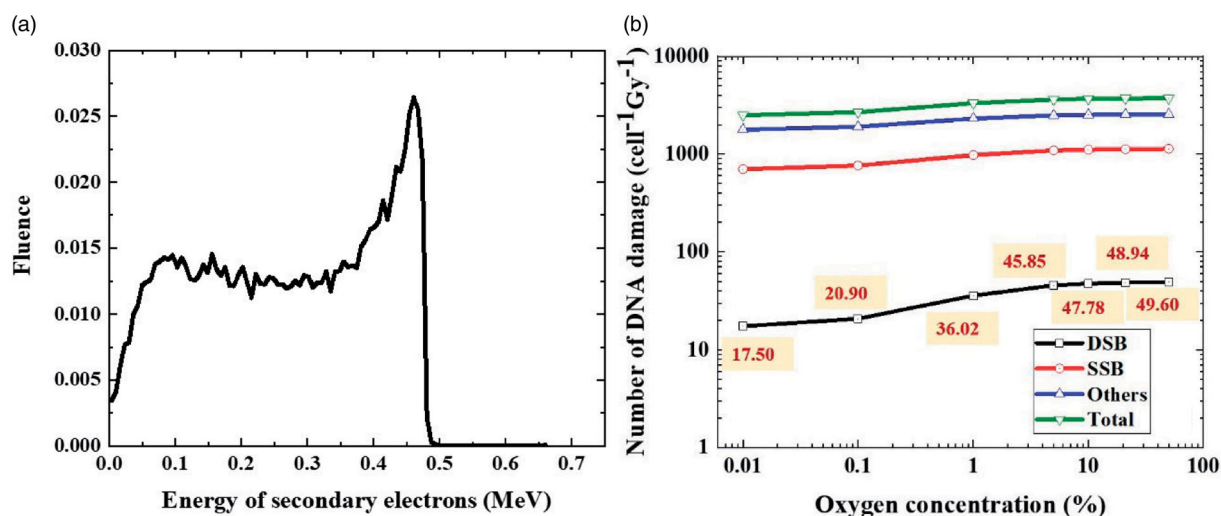
(a)

(b)

Figure 6. (a) Secondary electrons energy spectrum of ^{137}Cs; (b) yields of DNA damage caused by ^{137}Cs (reference radiation) under different oxygen concentrations.

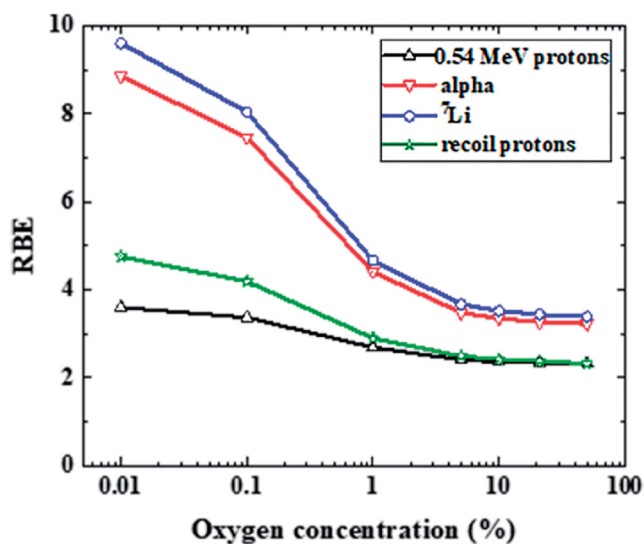**Figure 7.** RBE of a double-strand break created by all charged particles of BNCT relative to ^{137}Cs γ-rays at the different oxygen concentrations.

significant difference between hypoxic cells and normoxic cells. The effect of oxygen concentration must be considered in biological dose conversion and efficacy evaluation.

Calculation of the initial DNA damage and RBE caused by α and ^{7}Li particles based on boronophenylalanine (BPA)

For BPA, the weight distribution ratio of BPA in the nucleus, cytoplasm, cell membrane, and extracellular was 0:0.78:0:0.22 (Sato et al. 2018). Here, the distribution of BPA is set as the initial emission positions of α and ^{7}Li particles in the Geant4 simulation. The kinetic energy (Figure 8) is scored when the particles reach the surface of the nucleus.

As shown in Figure 9, the yields of BD and SSB caused by α particles are higher than that of ^{7}Li particles, and the profiles of other damages are lower than that of ^{7}Li particles. Similarly, the number of SSB, other damages, and total damages caused by α particles is significantly higher than those

of ^{7}Li particles. Furthermore, the RBE of α and ^{7}Li particles is 3.27 and 3.44, respectively.

Discussion

Accurate dose assessment and determination of the biological effectiveness of BNCT are challenging because of the complicated radiation types and energy distribution at the micro-nano scale (Streitmatter et al. 2020). In the present simulation study, considering the enrichment of boron in the tumor region and the sensitivity of cells, the effects of boron compounds distribution on DNA damage and biological effectiveness of α and ^{7}Li particles have been investigated. Moreover, the effects of oxygen concentration on DNA damage and RBE induced by all charged particles of BNCT are studied. Furthermore, BPA, a widely used boron compound in clinical application, is used to calculate the RBE of DSB induction of α and ^{7}Li particles at the normoxic conditions.

In the present study, when α or ^{7}Li particles are distributed in the cytomembrane or cytoplasm, the percentage of simple damages (BD and SSB) and other more complex damages (including SSB+, 2SSB, DSB, DSB+, and DSB++) has opposite trends in these two distributions. A possible explanation is when the particles are sampled in the cytomembrane, the average energy incident into the cell nucleus is lower than that in the cytoplasm, the range of particles in the cell nucleus is also different accordingly. Many previous studies have shown that the low-energy and high-LET particles could result in more complex DNA damages (Höglund et al. 2000; Hada and Georgakilas 2008; de la Fuente Rosales et al. 2018).

In traditional radiotherapy, the effect of cellular oxygen environment on DNA damage has been widely studied as the tumor is very often in a hypoxic environment. These results also proved that the change of oxygen concentration had a significant effect on DNA damage and even biological effectiveness (Stewart et al. 2011; Stewart 2019; Luo et al. 2020). As mentioned in the results section, the biological damage caused by α and ^{7}Li particles is almost not affected
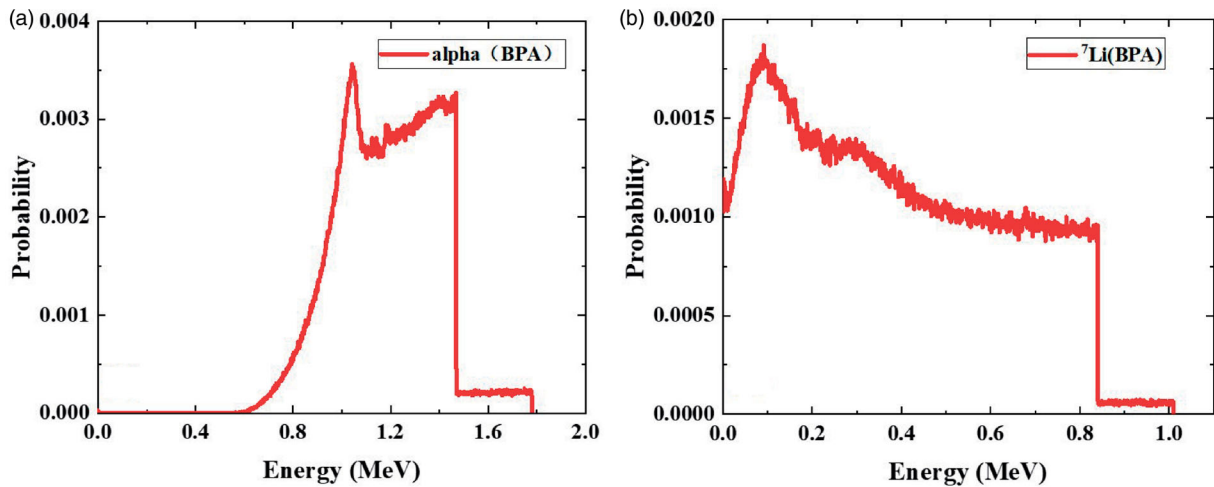
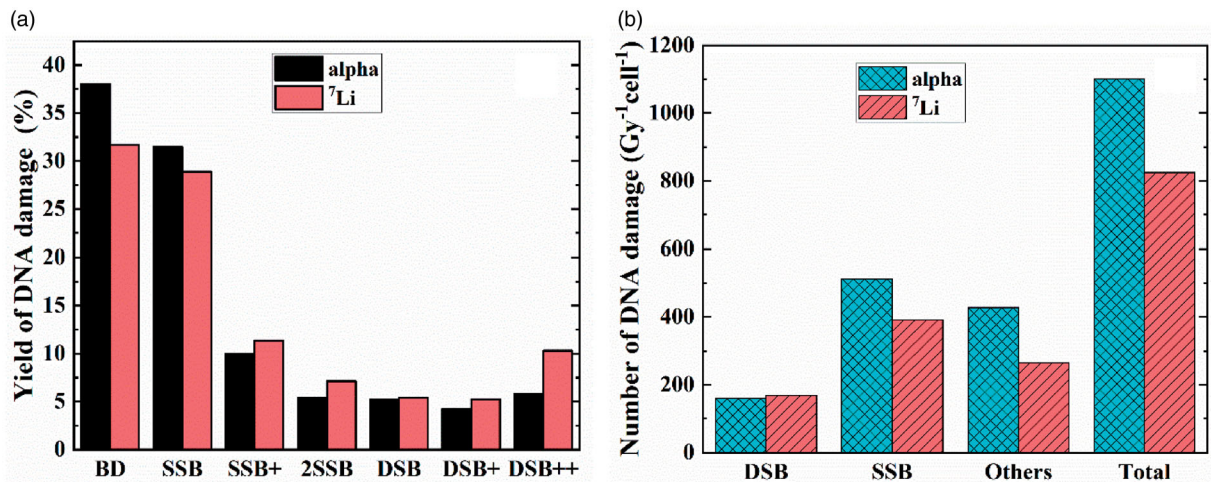**Figure 8.** Energy spectral distribution of α particles (a) and ^{7}Li particles (b) on the surface of the cell nucleus.

Figure 9. Percentage of DNA damage with different complexities (a) and number of clustered damage (b) caused by α and ^{7}Li particles based on BPA under normoxic conditions.

by the change of oxygen concentration. The main reason was that high-LET particles primarily caused DNA damage through direct action (Boucher et al. 2006), whereas oxygen concentration has a more significant impact on indirect action usually by photons. Notably, the number of clustered DSB obtained in our study is not in good agreement with that of Margis et al. (Margis et al. 2020). They considered clustered DSB as DSB++ and DSB+, whereas this study considers DSB types with three different complexities (DSB++, DSB+, and DSB) (Ou et al. 2018). For protons and recoil protons, corresponding to the neutron dose component of BNCT, when the boron concentration was 0, the RBE measured by the tissue-equivalent proportional counter (TEPC) was about 3.7, and the RBE obtained from the PHITS simulation by recording yd(y) range of 0.01–1000 keV/μm was about 3.0 (Hu, Tanaka, Takata, Okazaki, et al. 2020). However, in this study, it can be found that the RBE of single-energy protons and recoil protons decreases with the increase of oxygen concentration, from 5 to 2, which might be due to the difference in oxygen concentration in the tumor cells or environment and neutron flux. Moreover, compared with the results of 0% oxygen

concentration, at 50% oxygen concentration, the increase of clustered DSB induced by recoil protons is 49.42%, whereas the increase of clustered DSB induced by 0.54 MeV protons is 85.35%. A possible reason is that the average energy of recoil protons is higher than 0.54 MeV, and their average LET is lower than that of 0.54 MeV protons. Previous studies have shown that the low-LET radiations primarily caused individual DNA damage (Hong et al. 2016), and the relative yields of complex damage decreased with the decrease of oxygen concentration, thereby reducing the complexity of DNA damage.

When O_2 concentration was 21%, the number of DSB induction was about 8.1 Gy^{-1} Gbp^{-1} under the radiation of ^{60}Co (Luo et al. 2020), there were 8.16 DSBs in the estimation of the MCDS for a representative mammalian cell irradiated by ^{137}Cs x-rays (Stewart et al. 2011). In the current study, for the reference photon radiation, the simulated number of DSB induction is 48.94 Gy^{-1} cell^{-1}, which is consistent with the results of previous studies (Stewart et al. 2011). In addition, the number of SSBs, DSBs, other damages, and total damages induced by ^{137}Cs x-rays increases with the increase of oxygen concentration. According to

Equation 1, this result leads to the decrease of RBE of α and ^{7}Li particles with the increase of oxygen concentration, which is consistent with the conclusions of previous studies (Stewart et al. 2011). Different from α and ^{7}Li particles, the number of other damages caused by reference photons is higher than that of SSB, because the indirect action of photons plays a leading role in DNA damage, and the primary factors affecting the indirect effect are chemical substances, such as free radicals (Friedland et al. 2003). The reactive oxygen species were highly reactive with DNA during indirect actions, which induced DNA damage by detaching the hydrogen atoms or adding reactions across the double bonds (Boguslaw 2011).

Furthermore, BPA, a commonly used boron compound, is used to analyze the effect of specific boron distribution on energy spectrum α and ^{7}Li particles, and then analyze the effect on DNA damage. As mentioned in the results section, RBE of α and ^{7}Li particles based on BPA is closer to that of α and ^{7}Li sampled in the cytoplasm, which is a slight difference from that of α and ^{7}Li sampled in the cytomembrane. The main reason is the presence of BPA affects the energy deposited in the nucleus, and the presence of BPA affects the particle types for neutron capture therapy. Tracy et al. reported distribution of cell sizes in their cell survival experiments (Tracy et al. 2015), and then nucleus diameters of 3–6 μm were assessed to calculate RBE$_{DSB}$ in MCDS+ MCNP simulation. The RBE$_{DSB}$ of 1.5 and 1.8 MeV α particles were 3.24 and 3.19, respectively (Streitmatter et al. 2020), which were basically consistent with the results in our study. In the present study, the results focus on the biological effects of tumor cells. For the surrounding normal tissues, the evaluation of biological effects should clarify the ratio of boron concentration between tumor and normal tissue. The RBE of α and ^{7}Li particles evaluated in this study are different from the CBE of boron compounds. At present, the CBE of BPA in the tumor was 3.8 for calculating the biological dose of BNCT (Coderre and Morris 1999; Farías et al. 2014), but it is promising to calculate the biological dose from α and ^{7}Li particles, respectively, and then add them to obtain the total biological dose. In the previous experimental studies, For M8 and Mel-J human melanoma cell lines, 1% cell survival fraction was used as a biological endpoint, and the CBE factors of BPA were 2.1 and 3, respectively (Rossini et al. 2015). In the study of Hamada et al., for 500 mg/kg BPA, the CBE was 3.45, and at 750 mg/kg, the CBE was 3.0 (Hamada et al. 2010; Masunaga et al. 2014). It can be found our findings are not in complete agreement with those of the experiments. The possible reasons for these differences are: on the one hand, the RBE of α and ^{7}Li particles are different from the concept of CBE, on the other hand, the neutron flux spectrum, cell line types and the selected biological endpoint are different.

This study has several limitations. The irradiation direction of particles and the shape of cells are still relatively ideal in the whole Monte Carlo simulation process, which might not be consistent with the actual situation in clinical treatment. However, the findings in our study can also provide some theoretical reference for the research and development of new boron compounds and their radiobiological effects in BNCT. For some more realistic situations, such as cell type and cell structure, this study may be further considered with other Monte Carlo simulation or numerical calculation models.

Conclusion

The initial DNA damage and RBE induced by charged particles in BNCT were investigated by considering the difference of boron compounds enrichment and the radiosensitivity of cells by combining with Geant4 and Monte Carlo Damage Simulation software. When the oxygen concentration changed from 0% to 50%, the RBE of 0.54 MeV protons and recoil protons varied from 5 to 2. Notably, the oxygen concentration could affect the enrichment of boron compounds, which would change the RBE of α and ^{7}Li particles in the radiation-sensitive region. These findings indicate that the RBE of different particles formed during BNCT might be affected by many factors, which should be considered in the development of new boron compounds, dose calculations and treatment planning.

Disclosure statement

No potential conflict of interest was reported by the author(s).

Notes on contributors

Jie Qi, is a MS student in the Department of Nuclear Science and Technology, Nanjing University of Aeronautics and Astronautics, Nanjing, China.

Changran Geng, is an Associate professor in the Department of Nuclear Science and Technology, Nanjing University of Aeronautics and Astronautics, Nanjing, China.

Xiaobin Tang, is a Professor in the Department of Nuclear Science and Technology, Nanjing University of Aeronautics and Astronautics, Nanjing, China.

Feng Tian, is a PhD student in the Department of Nuclear Science and Technology, Nanjing University of Aeronautics and Astronautics, Nanjing, China.

Yang Han, is a PhD student in the Department of Nuclear Science and Technology, Nanjing University of Aeronautics and Astronautics, Nanjing, China.

Huan Liu, is a MS student in the Department of Nuclear Science and Technology, Nanjing University of Aeronautics and Astronautics, Nanjing, China.

Yuanhao Liu, is a Professor in the Department of Nuclear Science and Technology, Nanjing University of Aeronautics and Astronautics, Nanjing, China.

Silva Bortolussi, is a Senior researcher in the Department of Physics, University of Pavia, Pavia, Italy.

Fada Guan, is an Assistant professor in the Department of Radiation Physics, Division of Radiation Oncology, The University of Texas MD Anderson Cancer Center, Houston, TX, USA.

ORCID

Fada Guan   http://orcid.org/0000-0001-8477-7391

References

Allison J, Amako K, Apostolakis J, Arce P, Asai M, Aso T, Bagli E, Bagulya A, Banerjee S, Barrand G, et al. 2016. Recent developments in Geant4. Nucl Instruments Methods Phys Res Sect A Accel Spectrometers, Detect Assoc Equip. 835:186–225.

Barth RF, Coderre JA, Vicente MGH, Blue TE. 2005. Boron neutron capture therapy of cancer: current status and future prospects. Clin Cancer Res. 11(11):3987–4002.

Boguslaw L. 2011. Hydroxyl radical and its scavengers in health and disease. Oxidative Med Cell Longev. 2011:809696.

Boucher D, Testard I, Averbeck D. 2006. Low levels of clustered oxidative DNA damage induced at low and high LET irradiation in mammalian cells. Radiat Environ Biophys. 45(4):267–276.

Chatzipapas KP, Papadimitroulas P, Emfietzoglou D, Kalospyros SA, Hada M, Georgakilas AG, Kagadis GC. 2020. Ionizing radiation and complex DNA damage: Quantifying the radiobiological damage using Monte Carlo simulations. Cancers. 12(4):799.

Coderre JA, Morris GM. 1999. The radiation biology of boron neutron capture therapy. Radiat Res. 151(1):1–18.

de la Fuente Rosales L, Incerti S, Francis Z, Bernal MA. 2018. Accounting for radiation-induced indirect damage on DNA with the Geant 4-DNA code. Phys Medica. 51:108–116.

deLara CM, Jenner TJ, Townsend KMS, Marsden SJ, O'Neill P. 1995. The effect of dimethyl sulfoxide on the induction of DNA double-strand breaks in V79-4 mammalian cells by alpha particles. Radiat Res. 144(1):43–49.

Farías RO, Bortolussi S, Menéndez PR, González SJ. 2014. Exploring boron neutron capture therapy for non-small cell lung cancer. Phys Medica. 30(8):888–897.

Frese MC, Victor KY, Stewart RD, Carlson DJ. 2012. A mechanism-based approach to predict the relative biological effectiveness of protons and carbon ions in radiation therapy. Int J Radiat Oncol Biol Phys. 83(1):442–450.

Friedland W, Jacob P, Bernhardt P, Paretzke HG, Dingfelder M. 2003. Simulation of DNA damage after proton irradiation. Radiat Res. 159(3):401–410.

Geng C, Tang X, Guan F, Johns J, Vasudevan L, Gong C, Shu D, Chen D. 2016. GEANT4 calculations of neutron dose in radiation protection using a homogeneous phantom and a Chinese hybrid male phantom. Radiat Prot Dosimetry. 168(4):433–440.

Guan F, Geng C, Carlson DJ, Ma DH, Bronk L, Gates D, Wang X, Kry SF, Grosshans D, Mohan R. 2018. A mechanistic relative biological effectiveness model-based biological dose optimization for charged particle radiobiology studies. Phys Med Biol. 64(1):015008.

Hada M, Georgakilas AG. 2008. Formation of clustered DNA damage after high-LET irradiation: A review. J Radiat Res. 49(3):203–210.

Hamada N, Imaoka T, Masunaga S-i, Ogata T, Okayasu R, Takahashi A, Kato TA, Kobayashi Y, Ohnishi T, Ono K, et al. 2010. Recent advances in the biology of heavy-ion cancer therapy. J Radiat Res. 51(4):365–383.

Hawkins RB. 1998. A microdosimetric-kinetic theory of the dependence of the RBE for cell death on LET. Med Phys. 25(7):1157–1170.

Hiratsuka J, Fukuda H, Kobayashi T, Karashima H, Yoshino K, Imajo Y, Mishima Y. 1991. The relative biological effectiveness of 10B-neutron capture therapy for early skin reaction in the hamster. Radiat Res. 128(2):186–191.

Höglund E, Blomquist E, Carlsson J, Stenerlöw B. 2000. DNA damage induced by radiation of different linear energy transfer: Initial fragmentation. Int J Radiat Biol. 76(4):539–547.

Hong BJ, Kim J, Jeong H, Bok S, Kim YE, Ahn GO. 2016. Tumor hypoxia and reoxygenation: the yin and yang for radiotherapy. Radiat Oncol J. 34(4):239–249.

Horiguchi H, Sato T, Kumada H, Yamamoto T, Sakae T. 2015. Estimation of relative biological effectiveness for boron neutron capture therapy using the PHITS code coupled with a microdosimetric kinetic model. J Radiat Res. 56(2):382–390.

Howard ME, Beltran C, Anderson S, Tseung WC, Sarkaria JN, Herman MG. 2017. Investigating dependencies of relative biological effectiveness for proton therapy in cancer cells. Int J Part Ther. 4(3):12–22.

Hsiao Y, Stewart RD. 2008. Monte Carlo simulation of DNA damage induction by x-rays and selected radioisotopes. Phys Med Biol. 53(1):233–244.

Hu N, Tanaka H, Takata T, Endo S, Masunaga S, Suzuki M, Sakurai Y. 2020. Evaluation of PHITS for microdosimetry in BNCT to support radiobiological research. Appl Radiat Isot. 161:109148.

Hu N, Tanaka H, Takata T, Okazaki K, Uchida R, Sakurai Y. 2020. Microdosimetric quantities of an accelerator-based neutron source used for boron neutron capture therapy measured using a gas-filled proportional counter. J Radiat Res. 61(2):214–220.

Incerti S, Kyriakou I, Bernal MA, Bordage MC, Francis Z, Guatelli S, Ivanchenko V, Karamitros M, Lampe N, Lee SB, others. 2018. Geant4-DNA example applications for track structure simulations in liquid water: A report from the Geant4-DNA Project. Med Phys. 45(8):722–739.

Kamp F, Carlson DJ, Wilkens JJ. 2017. Rapid implementation of the repair-misrepair-fixation (RMF) model facilitating online adaption of radiosensitivity parameters in ion therapy. Phys Med Biol. 62(13):N285–N296.

Karaoglu A, Arce P, Obradors D, Lagares JI, Unak P. 2018. Calculation by GAMOS/Geant4 simulation of cellular energy distributions from alpha and lithium-7 particles created by BNCT. Appl Radiat Isot. 132:206–211.

Kiger WS, III, Sakamoto S, Harling OK. 1999. Neutronic design of a fission converter-based epithermal neutron beam for neutron capture therapy. Nucl Sci Eng. 131(1):1–22.

Lin YC, Liu YH, Jiang SH, Liu HM, Chou WT. 2011. The refinement of dose assessment of the THOR BNCT beam. Appl Radiat Isot Incl Data Instrum Methods Use Agric Ind Med. 69(12):1834–1837.

Luo WR, Chen FH, Huang RJ, Chen YP, Hsiao YY. 2020. Effects of indirect actions and oxygen on relative biological effectiveness: estimate of DSB inductions and conversions induced by therapeutic proton beams. Int J Radiat Biol. 96(2):187–196.

Margis S, Magouni M, Kyriakou I, Georgakilas AG, Incerti S, Emfietzoglou D. 2020. Microdosimetric calculations of the direct DNA damage induced by low energy electrons using the Geant4-DNA Monte Carlo code. Phys Med Biol. 65(4):45007.

Masunaga S-i, Sakurai Y, Tanaka H, Tano K, Suzuki M, Kondo N, Narabayashi M, Nakagawa Y, Watanabe T, Maruhashi A, et al. 2014. The dependency of compound biological effectiveness factors on the type and the concentration of administered neutron capture agents in boron neutron capture therapy. Springerplus. 3(1):1–11.

McNamara A, Geng C, Turner R, Mendez JR, Perl J, Held K, Faddegon B, Paganetti H, Schuemann J. 2017. Validation of the radiobiology toolkit TOPAS-nBio in simple DNA geometries. Phys Medica. 33:207–215.

Morris GM, Coderre JA, Hopewell JW, Micca PL, Rezvani M. 1994. Response of rat skin to boron neutron capture therapy with p-

boronophenylalanine or borocaptate sodium. Radiother Oncol. 32(2):144–153.

Moss RL. 2014. Critical review, with an optimistic outlook, on boron neutron capture therapy (BNCT). Appl Radiat Isot. 88:2–11.

Nikjoo H, Goodhead DT, Charlton DE, Paretzke HG. 1991. Energy deposition in small cylindrical targets by monoenergetic electrons. Int J Radiat Biol. 60(5):739–756.

Okumura K, Kinashi Y, Kubota Y, Kitajima E, Okayasu R, Ono K, Takahashi S. 2013. Relative biological effects of neutron mixed-beam irradiation for boron neutron capture therapy on cell survival and DNA double-strand breaks in cultured mammalian cells. J Radiat Res. 54(1):70–75.

Ou H, Zhang B, Zhao S. 2018. Monte Carlo simulation of the relative biological effectiveness and DNA damage from a 400 MeV/u carbon ion beam in water. Appl Radiat Isot. 136:1–9.

Rossini AE, Dagrosa MA, Portu A, Saint Martin G, Thorp S, Casal M, Navarro A, Juvenal GJ, Pisarev MA. 2015. Assessment of biological effectiveness of boron neutron capture therapy in primary and metastatic melanoma cell lines. Int J Radiat Biol. 91(1):81–89.

Rothkamm K, Löbrich M. 2003. Evidence for a lack of DNA double-strand break repair in human cells exposed to very low x-ray doses. Proc Natl Acad Sci. 100(9):5057–5062.

Sakata D, Belov O, Bordage M-C, Emfietzoglou D, Guatelli S, Inaniwa T, Ivanchenko V, Karamitros M, Kyriakou I, Lampe N, et al. 2020. Fully integrated Monte Carlo simulation for evaluating radiation induced DNA damage and subsequent repair using Geant4-DNA. Sci Rep. 10(1):1–13.

Sakata D, Lampe N, Karamitros M, Kyriakou I, Belov O, Bernal MA, Bolst D, Bordage M-C, Breton V, Brown JMC, et al. 2019. Evaluation of early radiation DNA damage in a fractal cell nucleus model using Geant4-DNA. Phys Medica. 62:152–157.

Sato T, Masunaga SI, Kumada H, Hamada N. 2018. Microdosimetric modeling of biological effectiveness for boron neutron capture therapy considering intra- and intercellular heterogeneity in 10B distribution. Sci Rep. 8(1):988.

Semenenko VA. 2006. Fast Monte Carlo simulation of DNA damage formed by electrons and light ions. Phys Med Biol. 51(7):1693–1706.

Semenenko VA, Stewart RD. 2004. A fast Monte Carlo algorithm to simulate the spectrum of DNA damages formed by ionizing radiation. Radiat Res. 161(4):451–457.

Stewart RD. 2019. Induction of DNA damage by light ions relative to 60 Co γ-rays. Int J Part Ther. 5(1):25–39.

Stewart RD, Yu VK, Georgakilas AG, Koumenis C, Park JH, Carlson DJ. 2011. Effects of radiation quality and oxygen on clustered DNA lesions and cell death. Radiat Res. 176(5):587–602.

Streitmatter SW, Stewart RD, Moffitt G, Jevremovic T. 2020. Mechanistic modeling of the relative biological effectiveness of boron neutron capture therapy. Cells. 9(10):2302.

Tang N, Bueno M, Meylan S, Perrot Y, Tran HN, Freneau A, Dos Santos M, Vaurijoux A, Gruel G, Bernal MA, others. 2019. Assessment of radio-induced damage in endothelial cells irradiated with 40 kVp, 220 kVp, and 4 MV X-rays by means of micro and nanodosimetric calculations. Int J Mol Sci. 20(24):6204.

Tracy BL, Stevens DL, Goodhead DT, Hill MA. 2015. Variation in RBE for survival of V79-4 cells as a function of alpha-particle (helium ion) energy. Radiat Res. 184(1):33–45.

Zhu H, McNamara AL, McMahon SJ, Ramos-Mendez J, Henthorn NT, Faddegon B, Held KD, Perl J, Li J, Paganetti H, et al. 2020. Cellular response to proton irradiation: a simulation study with TOPAS-nBio. Radiat Res. 194(1):9–21.

Zhu H, Mcnamara AL, Ramos-Mendez J, Mcmahon SJ, Henthorn NT, Faddegon B, Held KD, Perl J, Li J, Paganetti H, Schuemann J 2020. A parameter sensitivity study for simulating DNA damage after proton irradiation using TOPAS-nBio. Phys Med Biol. 65(8):085015..